NeuroLoop Utilities – Model-Based Synthesis Guide

Written by Christopher Thomas – December 12, 2023.

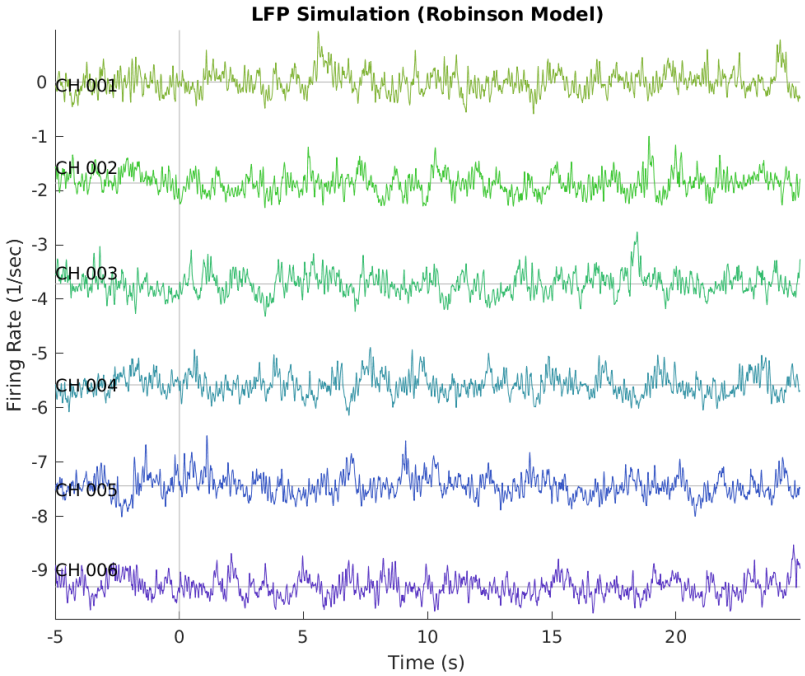

These files are part of the NeuroLoop project. This project is Copyright (c) 2018-2021 by Vanderbilt University, and is released under the Creative Commons Attribution 4.0 International License.

Contents

Chapter 1

Overview

This document describes the models used for synthesizing proxy neural activity using the "`nlSynth_`" family of library functions.

These functions are primarily intended to produce realistic-looking signals with known qualities to test analysis scripts with. That said, these models are drawn from publications where they were used to provide insight into the functioning of brain networks, so using these functions for such research is an additional use-case.

Chapter 2 describes the neural model presented in Robinson 2002 (and elaborated on in Freyer 2011 and Hindriks 2023). This is a model of average firing rates of multiple neural populations in the cortex and thalamus, with feedback connections that drive noise-excited oscillations.

FIXME: Other models go here once they're added.

Chapter 2

Robinson Model

The model presented in Robinson 2002 (hereafter "the Robinson model") provides a series of differential equations relating the firing rates of multiple neural populations in the cortex and thalamus. Feedback between these regions drives noise-excited oscillations.

The most relevant references are:

- Robinson 2002 – Describes the model, finds steady-state points, and analyzes perturbations around those points to find oscillation modes.
- Freyer 2011 – Describes an extension to the model where noise is modulated by the network's own output, providing a closer match to the distribution of oscillation modes in biological data.
- Hindriks 2023 – Describes an extension to the model that adds multiple independent copies of the Robinson and Freyer model, with coupling between instances. This is used to model co-oscillation of different brain regions in biological data.

(See Section 2.3 for citations.)

2.1 Model Description

A diagram of the Robinson model with the extensions from Freyer 2011 and Hindriks 2023 is shown in Figure 2.1. To distinguish this from the Robinson 2002 model, this will be referred to as "the extended Robinson model".

The neural population model is described in Equations 2.1, 2.2 and 2.3. Per Equation 2.1, a weighted sum of input firing rates $\phi_b(t)$ is used to generate the cell body potential $V_a(t)$. A single dot indicates the first time derivative, and a double dot indicates the second time derivative. The parameters α and β are the inverse of the membrane potential fall time and rise time, respectively. The coupling parameter ν_{ab} is the strength of the connection from region b to region a (zero if no connection, negative if inhibitory).

NOTE: A delay is manually applied to some of the ϕ_b signals before this summation to reflect signal propagation time between the cortex and thalamus (per Robinson 2002), and to reflect cross-coupling

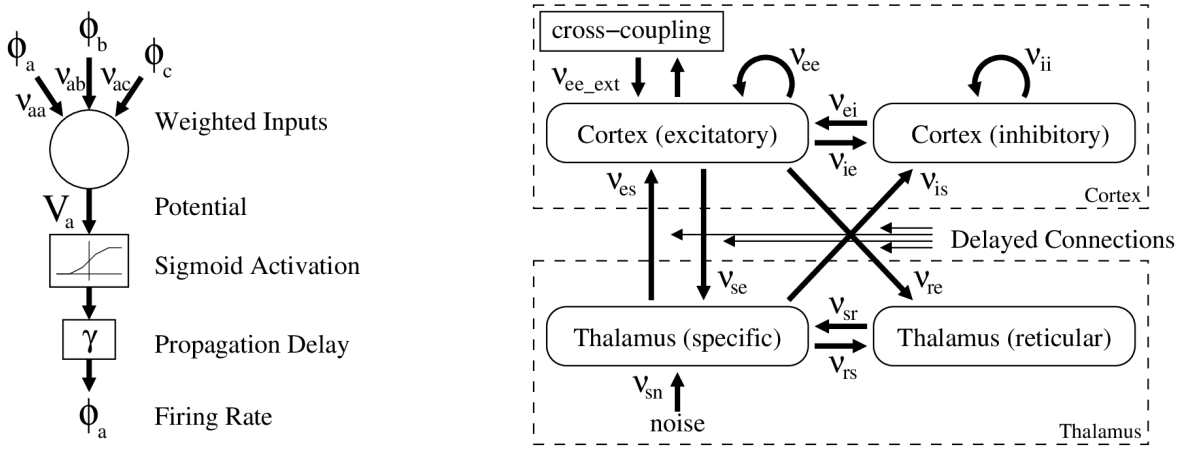

Figure 2.1: Extended Robinson model diagram, showing the neuron population model (left) and the population interactions (right).

delays within the cortex populations (per Hindriks 2023).

$$\left(\frac{1}{\alpha\beta}\right)\ddot{V}_a(t) + \left(\frac{1}{\alpha}+\frac{1}{\beta}\right)\dot{V}_a(t) + V_a(t) = \sum_b \nu_{ab}\phi_b(t) \tag{2.1}$$

Per Equation 2.2, the cell body potential V is fed into a sigmoid activation function, to represent the collective action of many neurons with varying firing thresholds. The mean firing threshold is V_{th} and the standard deviation of the threshold is σ_{th}. This follows the convention of Freyer 2011; Robinson 2002 defined a related parameter $\sigma'_{th} = \frac{\sqrt{3}}{\pi}\sigma_{th}$ to simplify the activation equation.

$$Q(V) = \frac{Q_{max}}{1 + e^{-\left(\frac{\pi}{\sqrt{3}}\right)\left(\frac{V-V_{th}}{\sigma_{th}}\right)}} \tag{2.2}$$

Per Equation 2.3, the local firing rate Q is propagated with damping and finite delay to give the non-local firing rate ϕ. A single dot indicates the first time derivative, and a double dot indicates the second time derivative. Per Robinson 2002, local propagation delay is assumed to only be relevant within the cortex, and $\gamma = \infty$ is assumed elsewhere. Per Freyer 2011, this further only applies to the excitatory neuron populations in the cortex.

$$\begin{cases} \frac{1}{\gamma^2}\ddot{\phi}(t) + \frac{2}{\gamma}\dot{\phi}(t) + \phi(t) = Q(t) & \text{Cortex excitatory neurons.} \\ \phi(t) = Q(t) & \text{All other populations.} \end{cases} \tag{2.3}$$

Noise is injected into the model as ϕ_n, and is described by Equation 2.4. Per Freyer 2011, there are three components: constant, additive, and multiplicative. Multiplicative noise (noise modulated by ϕ_e) is important for broadening the distribution of peak power levels of transient oscillations at frequencies above the fundamental oscillation mode of the cortex/thalamus loop.

In Equation 2.4, ϕ_n is the noise coupled to the thalamus via ν_{sn}, μ_n is the constant noise component (background firing rate), σ_n is the standard deviation of the independent component of the noise, and

χ is a scaling parameter (per Freyer 2011) such that $\sigma_n\chi$ is the standard deviation of the component of the noise that is modulated by ϕ_e. Since the ϕ_e signal has to propagate from the cortex to the thalamus before modulating this noise component, it is manually delayed. The signals $g_1(t)$ and $g_2(t)$ denote two independent Gaussian noise sources with zero mean and with standard deviations of 1.

$$\phi_n(t) = \mu_n + \sigma_n g_1(t) + \sigma_n \chi g_2(t)\phi_e(t - t_{halfloop}) \tag{2.4}$$

As shown in Figure 2.1, cross-coupling between excitatory cortical populations is implemented per Hindriks 2023. This is described by Equation 2.5. Weight values w_{ab} represent the strength of connections between populations, and delay values $t_{coupling_{ab}}$ represent the propagation delays of these connections. While arbitrary weight values may be chosen, the recommended implementation is to use positive weights (purely excitatory), with the constraint that the sum of all weights contributing to a given ϕ_{ext_k} should sum to approximately unity. Cross-coupling propagation delay is typically no more than $\frac{1}{\gamma}$.

$$\phi_{ext_a}(t) = \sum_b w_{ab}\phi_e(t - t_{coupling_{ab}}) \tag{2.5}$$

$$\forall a, \sum_b w_{ab} \approx 1 \tag{2.6}$$

Typical parameter values for the extended Robinson model are shown in Table 2.1. Typical coupling coefficients are shown in Table 2.2. These are very similar to the parameter and coupling coefficient values used in Hindriks 2023.

Parameter	**Value**	**Units**	**Notes**
Q_{max}	250	sec^{-1}	maximum firing rate
V_{th}	15	mV	potential threshold for firing
σ_{th}	6	mV	standard deviation of firing threshold
α	50	sec^{-1}	membrane potential inverse fall time
β	200	sec^{-1}	membrane potential inverse rise time
γ	100	sec^{-1}	cortex inverse propagation delay
$t_{halfloop}$	40	ms	one-way cortex/thalamus delay
μ_n	0	sec^{-1}	constant noise firing rate
σ_n	0.1	sec^{-1}	additive noise standard deviation
χ	0.3	dimensionless	multiplicative noise deviation coefficient

Table 2.1: Typical parameters for the extended Robinson model.

ν_{ee}	1.2
ν_{ei}	-1.8
ν_{es}	1.2
ν_{ie}	1.2
ν_{ii}	-1.8
ν_{is}	1.2
ν_{se}	1.2
ν_{re}	0.4
ν_{sr}	-0.8
ν_{rs}	0.2
ν_{sn}	0.5
$\nu_{ee_{ext}}$	0.07

Table 2.2: Typical coupling coefficient values for the extended Robinson model.

2.2 Discussion

Applying the Laplace transform to Equation 2.1 shows that the effect of α and β is to apply a low-pass filter to the weighted sum of input firing rates (a second-order exponential smoothing filter with poles at $-\alpha$ and $-\beta$).

$$\left(\frac{1}{\alpha\beta}\right) s^2 V_a(s) + \left(\frac{1}{\alpha} + \frac{1}{\beta}\right) s V_a(s) + V_a(s) = \sum_b \nu_{ab} \Phi_b(s) \tag{2.7}$$

$$s^2 V_a(s) + (\alpha + \beta) s V_a(s) + \alpha\beta V_a(s) = \alpha\beta \sum_b \nu_{ab} \Phi_b(s) \tag{2.8}$$

$$(s + \alpha)(s + \beta) V_a(s) = \alpha\beta \sum_b \nu_{ab} \Phi_b(s) \tag{2.9}$$

$$\frac{V_a(s)}{\sum_b \nu_{ab} \Phi_b(s)} = \frac{\alpha\beta}{(s + \alpha)(s + \beta)} \tag{2.10}$$

Applying the Laplace transform to Equation 2.3 shows that the effect of γ is to apply a low-pass filter to the firing rate (a second-order exponential smoothing filter with both poles at $-\gamma$).

$$\left(\frac{1}{\gamma^2}\right) s^2 \Phi(s) + \left(\frac{2}{\gamma}\right) s \Phi(s) + \Phi(s) = Q(s) \tag{2.11}$$

$$s^2 \Phi(s) + 2\gamma s \Phi(s) + \gamma^2 \Phi(s) = \gamma^2 Q(s) \tag{2.12}$$

$$(s + \gamma)^2 \Phi(s) = \gamma^2 Q(s) \tag{2.13}$$

$$\frac{\Phi(s)}{Q(s)} = \frac{\gamma^2}{(s + \gamma)^2} \tag{2.14}$$

The fundamental-mode oscillation is usually supported by resonance in the cortico-thalamic loop, with a period near $2 \cdot t_{halfloop}$ (alpha band for $t_{halfloop}$ of 40 ms). The first overtone mode can support beta band oscillations. If coupling values are chosen such that the system is only barely stable near these resonance modes, oscillatory bursts can occur.

Robinson 2002 gives a detailed description of how this stability analysis may be performed. For some regions of parameter space, multiple operating points exist. With parameter values chosen from these regions, the system will switch between several states with different oscillation characteristics. The parameter values used in Freyer 2011 and Hindriks 2023 were chosen to exploit this behavior.

2.3 References

- P. A. Robinson, C. J. Rennie, and D. L. Rowe, *Dynamics of Large-Scale Brain Activity in Normal Arousal States and Epileptic Seizures*, Physical Review E, 65, 041924, April 2002
- F. Freyer, J. A. Roberts, R. Becker, P. A. Robinson, P. Ritter, and M. Breakspear, *Biophysical Mechanisms of Multistability in Resting-State Cortical Rhythms*, Journal of Neuroscience, 31, pp 6353–6361, April 2011

- R. Hindriks and P. K. B. Tewarie, *Dissociation Between Phase and Power Correlation Networks in the Human Brain is Driven by Co-Occurrent Bursts*, Communications Biology, 6, 286, March 2023